BURNED AREA DETECTION USING HIGH SPATIAL RESOLUTION 4 BANDS TRIPLESAT IMAGERY

Min Er Nah*[1], Chong Chen[1], Bin Zhou[1], Ting Chen[2], Jianjun He[2]

[1]Twenty First Century Aerospace Technology (Asia) Pte. Ltd., 61 Science Park Road, #05-17 The Galen, Singapore Science Park II, Singapore 117525
[2]Twenty First Century Aerospace Technology Co., Ltd., No. 26 Jiancaicheng East Road, Haidian District, Beijing 100096, China
Email: miner.nah@21at.sg; chenchong@21at.sg; zhoubin@21at.sg; chenting@21at.com.cn; hejj@21at.com.cn

KEY WORDS: TripleSat, Burned area detection, Spectral indices, High resolution, Satellite images

ABSTRACT: With the increase in forest fires over the years due to global warming and anthropogenic actions, large scale burned area detection is necessary for damage control, reforestation and reconstruction projects. This is especially so for forests near populated areas. Remote sensing using satellite images has proven to be a useful tool for extensive coverage of burned area monitoring. However, detection of small burned areas (< 50 ha) is limited for open sourced medium to coarse resolution satellite images. High resolution satellite images with < 1 m spatial resolution can improve the accuracy in detecting these burned areas.

TripleSat imagery has a high spatial resolution of 0.8 m and a swath width of 23.8 km. It consists of four bands, namely blue, green, red, and near infrared (NIR). The spectral band wavelength range from 440 to 910 nm. With its high spatial resolution and multispectral bands, finer details such as individual houses and small groups of forest stands can be clearly differentiated in a large region of interest, making these images very useful for targeted ground observation projects like burned area detection. Although most commonly used burned area indices such as Normalized Burn Ratio (NBR), Normalized Burn Ratio2 (NBR2), Burned Area Index Modified with short SWIR band (BAIMs), and Char Soil Index (CSI) require short wave infrared band (SWIR), in the absence of high spatial resolution short wave infrared band, a method using TripleSat images' four bands to detect burned areas was proposed.

In this study, two pairs of TripleSat images were used to detect burned area for two different locations in New South Wales, Australia. In order to compare the before and after changes due to the 2019 to 2020 bushfire season in Australia, the first pair of images was taken in May 2018 and February 2020 and the second pair of images was taken in April 2016 and February 2020. The workflow consists of five steps: 1) vegetation extraction, 2) seed pixel generation, 3) threshold calculation, 4) region growing segmentation and 5) post processing. First, vegetation areas were extracted using Normalized Difference Vegetation Index (NDVI). Next, the Global Environmental Monitoring Index (GEMI), Burn Area Index (BAI), NIR and red bands that are highly sensitive to burned areas were utilized to find burned area seed pixels. Adaptive thresholds based on the cumulative distribution function of burned and unburned pixels were calculated in the following step. In step 4, region growing segmentation was implemented to separate burned and unburned areas. Last, post processing was performed on the segmented results. According to the results, more than 95% of the burned areas can be detected and an estimated 93 km^2 of burned area were detected in the study regions. This study shows that high spatial resolution (0.8m) 4 bands TripleSat images are capable of extracting large and small burned areas in the region of interest.

1. INTRODUCTION

Forests help to regulate the climate by providing a carbon sink that absorb 2.4 billion metric tons of carbon per year. Over 1.6 billion people are dependent on forests for food or fuel sources and nearly 70 million people worldwide reside among forests. Forests can prevent soil erosion, acting as a buffer for local communities against natural disasters like landslides and floods (WWF, 2020). Yet, forest fires are threatening the survival of these forests. Forest fires can occur from natural causes like lightning and from anthropogenic actions like unauthorised human-caused fires and escaped fires from prescribed burn projects (Hoover & Hanson, 2023). Forest degradation and agricultural expansion are one of the most common anthropogenic causes of forest fires (WWF, 2020). Over the past decade, forest fires are worsening with higher occurrence rates, greater severity and wider spatial extents (MacCarthy et al, 2023). Climate change is also exacerbating the situation as the high inter annual climate variability such as prolonged droughts and decreased rainfall has increased the danger of fire activity (Canadell et al, 2021). As a result, total burned area is increasing quite significantly over the years. Tree cover lost due to forest fires are estimated to be 3 million hectare more per year as compared to 2001 globally and accounted for more than a quarter of all tree cover loss over the past 20 years (MacCarthy et al, 2023). Burned area detection is thus crucial for the calculation of tree cover loss and assessing the severity of forest

damage. The data may help mitigate forest fires' impacts to prevent forest depletion as well as aiding forest recovery. Tracking burned areas can help identify trends and patterns of fire occurrence, investigate drivers of fire occurrence, predict future fire pattern behavior and assess fire impact on the natural system (USGS, 2023).

Remote sensing using satellite images play an essential role in tracking burned area as satellite images can cover a wide extent in a timely manner as well as covering geographic locations that may not be easily accessible by vehicles. A variety of burned area products derived from satellite images with various spatial resolutions are available online like MODIS Burned Area Product (500m resolution), FireCCI51 (250m resolution), and Landsat Level 3 Burned Area Science Product (30m resolution). Burned area indices like Normalized Burn Ratio (NBR), Burned Area Index Modified with short SWIR band (BAIMs), and Char Soil Index (CSI) are also available to calculate burned area in a study region of interest using open sourced satellite images like Sentinel 2, Sentinel 3, Landsat and MODIS. These products may be of a coarser resolution, ranging from 500m to 10m resolution but are able cover a great extent in a timely manner. Different papers used these data and algorithms to detect burned areas with varying extents (Stroppiana et al, 2012; Chuvieco et al, 2019; Lizundia-Loiola et al, 2020). However, due to the medium to coarse resolution, accuracy of detecting small burned areas is reduced (Campagnolo et al, 2021). Zubieta (2023) also stated that there were high omission errors in the detection of small burned areas less than 50 ha using MODIS or VIIRS heat spots in Andean ecosystems of Cusco, Peru**.** These burned area products may not provide enough details if an in depth study on the effects of fire at the regional or local scale is required. Especially for forests near populated areas, more details in the images may be needed like houses and small groups of forest stands to understand how the burned area may impact forest biodiversity and livelihoods of people dependent on the forests eg tourism and logging industry. Llorens et al (2021) used Sentinel 2 data to estimate the extent of burned areas affected by forest fires for October 2017 fires in the Iberian Peninsula. The authors found that using higher spatial resolution images like Sentinel 2 with 10 and 20m resolution as compared to MODIS images with 250m resolution improves the area estimate by 10% in commission area. High resolution satellite images with < 1 m spatial resolution can be an alternative solution to improving the accuracy in detecting small burned areas by providing more spectral details in the images.

Most commonly used burned area indices for remote sensing such as Normalized Burn Ratio (NBR), Normalized Burn Ratio2 (NBR2), Burned Area Index Modified with short SWIR band (BAIMs), and Char Soil Index (CSI) all utilise the short wave infrared band to detect burned areas. Short wave infrared bands (SWIR) and near infrared bands (NIR) are very useful in detecting burned areas as newly burned areas affect these wavelengths strongly (Pleniou & Koutsias, 2013) but SWIR band is not found in most high resolution satellite images. However, burned area detection can be categorised as a type of change detection as the aim is to compare how the land has changed before and after the occurrence of forest fires using the spectral differences captured in satellite images. High resolution 4 bands satellite images have been proven useful in several vegetation change detection studies (Gärtner et al, 2014; Uddin el al, 2015; Panuju et al, 2020). For small burned areas (< 50 ha), high spatial resolution satellite images may be more useful in detecting these changed vegetation areas. From this point of view, high resolution 4 bands satellite images can substitute as input data too by using the NIR band for burned area detection. The aim of this paper is to propose a method using high spatial resolution 0.8m TripleSat images' 4 bands to detect burned areas. Two pairs of images taken in February 2020 will be used to detect burned areas caused by the 2019 to 2020 forest fires in New South Wales, Australia. The paper will be separated into five sections: 1) introduction, 2) study areas and data, 3) methodology, 4) results and discussion and 5) conclusion. Section 1 will provide an introduction on burned area detection using satellite images and Section 2 will describe the selected data and study

a) Location of study areas in NSW, Australia b) Location of study areas overlaid on google map

Figure 1. Location of study areas

areas. The algorithms used in detecting burned areas will be further explained in Section 3. Section 4 will showcase the results and section 5 will conclude this paper.

2. STUDY AREAS & DATA

2.1. Study Areas

The study areas chosen for this paper are located in New South Wales (NSW), Australia (Figure 1a). It was one of the worst hit areas during the 2019 to 2020 bushfire season where 5.5 million hectare of land was burned. Over 300,000 hectares or 37% of all NSW rainforest was burned during the 2019–20 fire season (NSW EPA, 2021). Study area 1 is located near Conjola Lake with latitude 35.2624° S, and longitude 150.4631° E and study area 2 is located near Malua Bay with latitude 35.7930° S and longitude 150.2169° E (Figure 1b). A pair of images was selected for each study area to compare before and after changes in the burned areas. The first pair of TripleSat 0.8m resolution images was taken on 06th May 2018 (Figure 2a) and 25th February 2020 (Figure 2c) for study area 1 and the second pair of TripleSat 0.8m

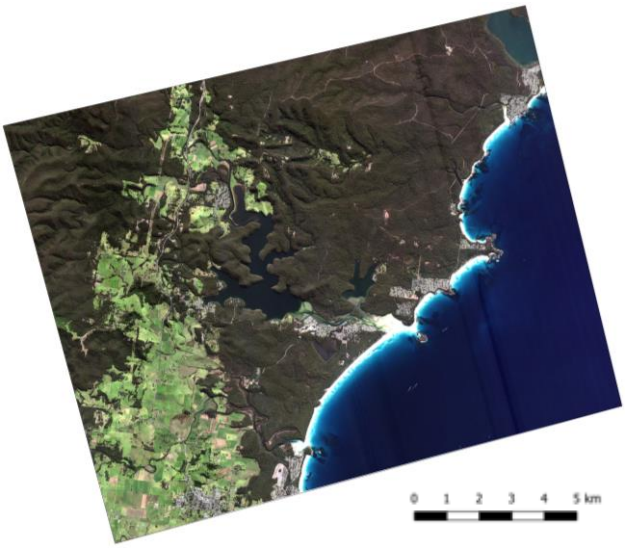

a) Study Area 1: Reference image taken on 06th May 2018

b) Study Area 2: Reference image taken on 20th April 2016

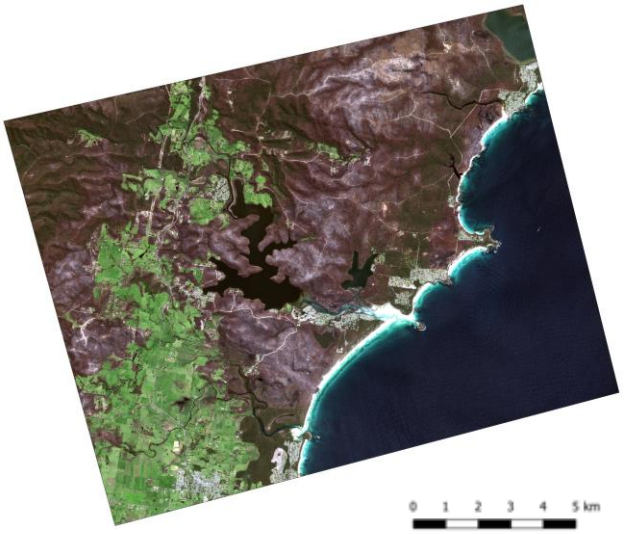

c) Study Area 1: Target image taken on 25th February 2020

d) Study Area 2: Target image taken on 20th February 2020

Figure 2. TripleSat images of study areas

Table 1. Spectral bands available in TripleSat Imagery

Spectral Bands	Spectral Band Wavelengths (nm)
Panchromatic	450 to 650
Blue	440 to 510
Green	510 to 590
Red	600 to 670
Near infrared	760 to 910

resolution images was taken on 20th April 2016 (Figure 2b) and 20th February 2020 (Figure 2d) for study area 2. Figure 2a and c covered an area of 229.3 km^2 and Figure 2b and d covered an area of 114.5 km^2.

2.2. Data

The TripleSat Constellation consists of three identical optical satellites align in the same orbital plane, 120° apart. This allows it to target anywhere on Earth once per day. The satellites move in a sun synchronous circular direction at an altitude of 651km. The spectral bands available are in 0.8m resolution panchromatic band and 3.2m resolution multispectral bands, namely blue, green, red, and near infrared (NIR) (21AT, 2023). The spectral band wavelengths range from 450nm to 910 nm (Table 1). TripleSat pan sharpened multispectral images can thus be categorised as high resolution images with spatial resolution of 0.8m and a swath width of 23.8km. With its high spatial resolution and multispectral bands, finer details can be clearly differentiated in a large region of interest, making these images very useful for targeted ground observation projects like burned area detection. TripleSat images have been used in several studies like emergency monitoring and post disaster reconstruction monitoring (Cui et al, 2020), object detection (Qi, 2022) and tree cover classification (Guliaeva et al, 2021). Level 4 TripleSat images that were pan-sharpened and ortho-rectified were used in this paper.

3. METHODOLOGY

3.1. Workflow

The workflow (Figure 3) consists of five steps: 1) vegetation extraction, 2) seed pixel generation, 3) threshold calculation, 4) region growing segmentation and 5) post processing. First, vegetation areas are extracted using Normalized Difference Vegetation Index (NDVI) to find potential forest areas in the image taken before fire occurrence. Next, the Global Environmental Monitoring Index (GEMI), Burn Area Index (BAI), NIR and red bands that are highly sensitive to burned areas are utilized to find burned area seed pixels otherwise known as the initial fire spots in the image taken after fire occurrence. Adaptive thresholds based on the cumulative distribution functions of burned and unburned pixels are calculated in the following step. In step 4, region growing segmentation is implemented to separate burned and unburned areas since burned areas tend to spread outwards from the initial reference point. Last, post processing is performed on the segmented results.

3.2. Retrieval of valid vegetation areas

Burned areas will be detected in the more recent images taken in February 2020 and will be labelled as the target images henceforth (Figure 2c and 2d). The earlier images will be labelled as the reference images (Figure 2a and 2b). The satellite images will first undergo normalization and stretching for optimum contrast. In order to find burned areas in forests only, areas that are not forest in both the reference and target images eg water and urban areas need to be removed. First, the Normalised Difference Water Index (NDWI) (Equation 1) is calculated for the reference and target images to create a

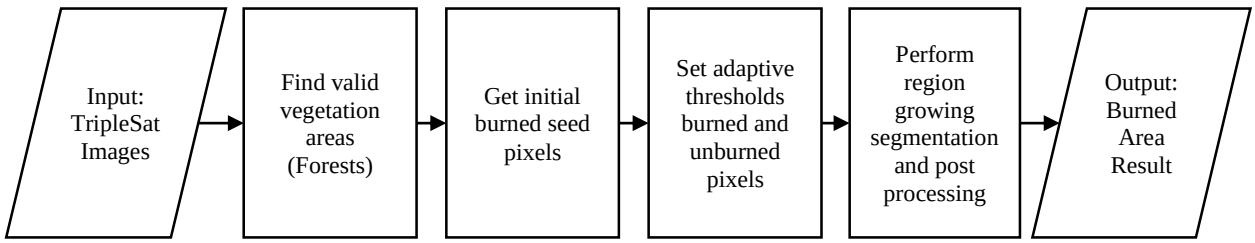

Figure 3. Workflow

water mask. Pixels that have high NDWI values in both reference and target images will be labelled as water as high NDWI values indicate presence of water.

$$NDWI = \frac{Green - NIR}{Green + NIR} \quad (1)$$

Next, urban areas tend to be brighter than vegetation and burned areas. Thus, a lightness mask is created using LAB images. If pixels have high lightness values in the reference or target images, they will be deemed as urban areas.

Normalised Difference Vegetation Index (NDVI) (Equation 2) is also calculated for both reference and target images to get the vegetation masks representing forests for reference and target images. Areas that have high NDVI values in the target image will be removed since these areas were unburned.

$$NDVI = \frac{NIR - Red}{NIR + Red} \quad (2)$$

The remaining pixels that are not in the water mask or the building mask and do not have high NDVI values in the target image will be the valid pixels used in the burned area detection process. Burned vegetation show a strong decrease in NIR due to lower leaf area index or reduction in leaf pigment when leaves get burned or even desiccation when leaves get scorched (Chuvieco et al, 2019). Since the NIR band is sensitive to recent burns, areas with low near infrared values can be classified as potential burned areas. Spectral indices like the Global Environmental Monitoring Index (GEMI) and the Burn Area Index (BAI) will be utilised too. GEMI (Equation 3) is a non-linear index that has been proven useful for detecting burned areas using the red-near infrared space (Pereira, 1999). BAI (Equation 4) utilises the NIR and red bands to distinguish fire affected areas based on spectral distance of each pixel to a reference spectral point that burned areas tend to converge to (Chuvieco et al, 2002).

$$GEMI = n(1 - 0.25n) - \frac{Red - 0.125}{1 - Red} \quad (3)$$

$$where\ n = \frac{2(NIR^2 - Red^2) + 1.5(NIR) + 0.5(Red)}{Red + NIR + 0.5}$$

$$BAI = \frac{1}{(0.1 - Red)^2 + (0.06 - NIR)^2} \quad (4)$$

GEMI (Equation 3) and BAI (Equation 4) will be calculated using the remaining pixels for both reference and target images. A GEMI maximum difference mask is also required to use the difference in vegetation values to verify vegetation changes.

3.3. Generation of seed pixels

Burned pixels are defined as healthy green vegetation areas in the reference image but non vegetation areas (desiccated vegetation) in the target image. Thus, initial burned seed pixels for region growing segmentation will be defined as pixels with low NDVI values in the target image and higher NDVI in the reference image. Pixels must also have low NIR values and have a larger difference from the reference image.

After the above step, the initial seed pixels will undergo a second check to ensure that it can be categorised as a valid burn pixel using the NIR values of the target image and the distribution of seed pixels. Based on experiments and with reference to the criteria used in Lizundia-Loiola et al (2020), a potential burned seed pixel is more likely to be the pixel that has minimum NIR value within a suitable distance buffer surrounding each initial seed pixel. Therefore, using a window surrounding each seed pixel, the minimum NIR value and the pixel location will be saved in a new burned seed pixels mask. The unburned pixels mask will consist of the remaining pixels that are not within the distance buffer surrounding each seed pixel. The same pixel locations in the burned and unburned pixel mask will then be used to retrieve the corresponding GEMI values, BAI values, red values and GEMI difference values. These values will be utilised to calculate statistics for burned and unburned pixels to find adaptive thresholds in the next step.

3.4. Calculation of adaptive thresholds

Region growing segmentation works by iteratively growing each seed pixel until the pixel no longer fulfils the set criteria. Adaptive thresholds to set the criteria can be defined by using the available statistics. Cumulative distribution function is used to describe the probability distribution of random variables, in this case the probability that the burned or unburned pixel will take a certain value. Therefore, it can assist to set adaptive thresholds instead of a fixed threshold. Cumulative distribution functions (CDF) for the burned seed pixels mask and unburned pixels mask are first calculated. Based on experiments, the NIR threshold for burned pixels can be defined as 10% of unburned pixels' CDF. CDFs will also be calculated using the same seed pixels to find adaptive thresholds for GEMI, BAI, red band and the GEMI difference to separate burned and unburned pixels.

3.5. Region growing segmentation

Subsequently, each burned seed pixel will undergo region growing segmentation by checking the NIR values of all its eight surrounding neighbours. If the pixel value is below the burned pixels' adaptive threshold and within the distance threshold, it will be considered as a burned pixel. Its 8 neighbours' values will continue to be analysed recursively until the NIR value is equal or larger than the burned pixels' adaptive threshold. A binary mask showing burned areas based on NIR values will be created. The same seed pixels will under region growing again using the GEMI mask to get a mask showing burned areas based on GEMI values. The following criteria will also be used to separate burned and unburned pixels.

a) Target image's red band < burned pixels' CDF threshold using red band
b) Target image's BAI > burned pixels' CDF threshold using BAI
c) GEMI difference > burned pixels' CDF threshold using GEMI difference

3.6. Post processing

Last, large polygons where the cumulated number of burned pixels greatly exceed the number of initial seed pixels in the neighbouring area need to be removed from the burned area result as it is not logical for a small fire to spread so far out. The burned area result will undergo connected component analysis and each connected component will be compared with the initial burned seed pixels mask. If the connected component is not within the distance buffer surrounding the seed pixels, it will be removed. Morphological functions will be applied to reduce the salt and pepper effect. The final result will be a binary mask where burned pixels will have the value 1 and unburned pixels 0.

4. RESULTS & DISCUSSION

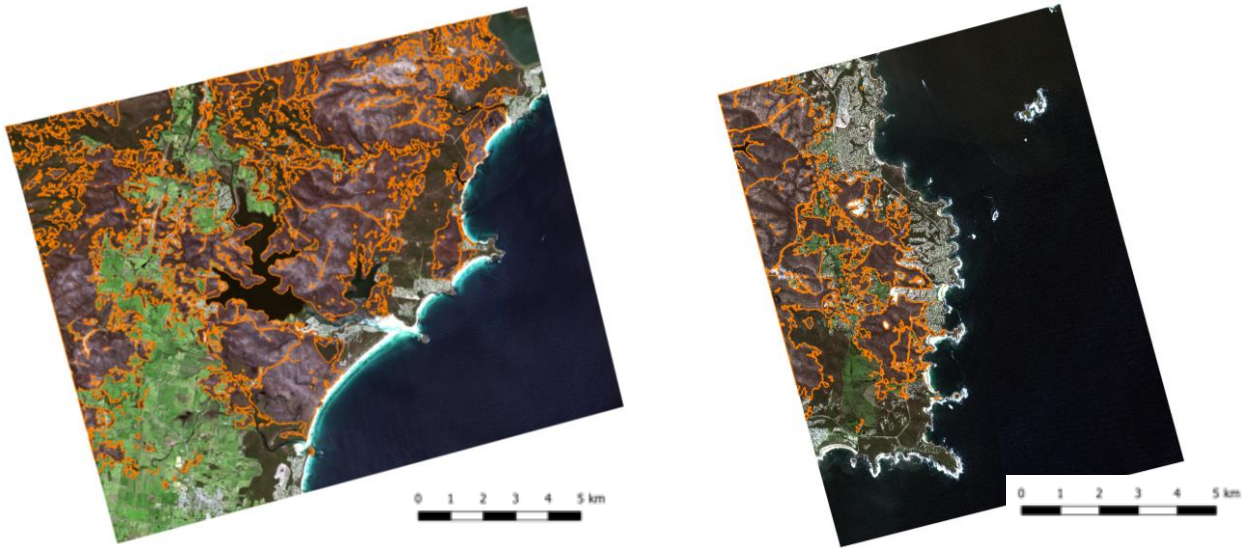

a) Burned area result for study area 1 on 25th February 2020 overlaid on TripleSat image

b) Burned area result for study area 2 on 20th February 2020 overlaid on TripleSat image

Figure 4. Burned areas results for study area 1 and 2

Table 2. Producer's accuracy and user's accuracy for study area 1 and study area 2

	Producer's Accuracy	User's Accuracy
Study Area 1	0.979	0.988
Study Area 2	0.987	0.984

Figure 4a and b show the burned area results outlined in orange for study area 1 and study area 2 respectively. An estimated 74.4 km^2 of burned area was detected in study area 1 located near Conjola Lake and an estimated 18.4 km^2 of burned area was detected for study area 2 located near Malua Bay. In study area 1, large burned areas were detected near the left side of the image and on the right side of Conjola Lake (Figure 5a). The results clearly outlined the various shades of brown desiccated vegetation. Patches of black carbon can also be seen in study region 1 using TripleSat's high resolution images (Figure 5b). Small patches of burned areas were detected near areas with houses in both study regions (Figure 5c and d) and these areas may be of interest to the local communities like fire protection services and insurance companies.

Validation of the proposed method is based on two points: 1) calculating producer's accuracy and user's accuracy using random points and 2) comparing TripleSat results with a burn area index (Normalised Burn Ratio) calculated using Sentinel 2 SWIR band. First, 10,000 random points were generated using QGIS random points tool and dispersed throughout each study area. More than 95% of the burned areas in study area 1 and study area 2 can be detected using TripleSat images (Table 2). This study shows that high spatial resolution (0.8m) 4 bands TripleSat images are capable of extracting large and small burned areas in the region of interest.

Second, Sentinel 2 images with SWIR band were utilised to calculate the Normalised Burn Ratio (NBR) to compare whether the short wave infrared (SWIR) band is necessary for burned area detection. Sentinel 2 images were taken on February 24th 2020 for study area 1 and study area 2. Low NBR values indicated by bright pixels in the image showed burned areas and dark pixels showed unburned areas. TripleSat results were able to clearly delineate the large bright burned regions in both study areas (Figure 6a and b). Compared to Sentinel 2 NBR results, small burned area polygons

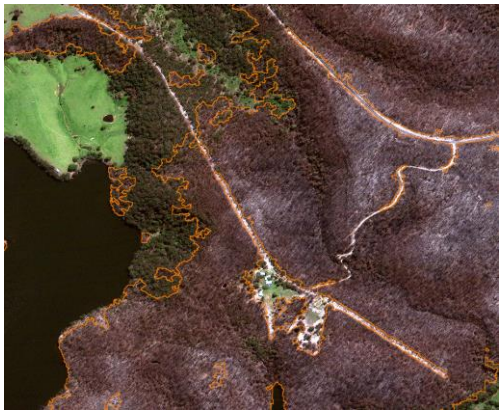

a) Close up view of the right side of Conjola Lake

b) Close up view of black patches that may be carbon

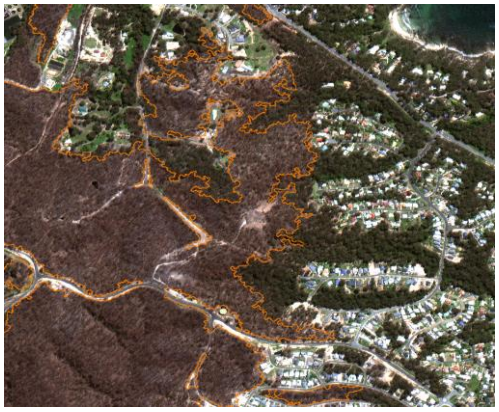

c) Close up view of burned areas near populated areas

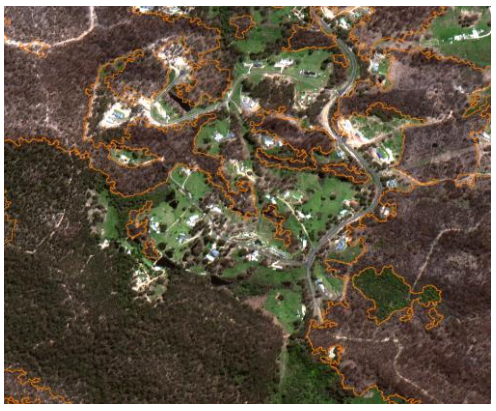

d) Close up view of burned areas near populated areas

Figure 5. Close up views of burned area result using TripleSat images

were more distinguishable in TripleSat's results (Figure 6c and d). This may indicate that spatial resolution does affect the accuracy in detecting smaller burned areas. Higher spatial resolution images (< 1m) without SWIR band can indeed be more useful in detecting small burned areas especially in study areas at the local scale.

5. CONCLUSION

In conclusion, this paper proposed a method to use high spatial resolution 4 bands 0.8m TripleSat imagery to detect burned areas. The method utilises a pair of TripleSat images and consists of five steps. Step 1 involves searching for potential forests areas by calculating NDVI using an earlier image taken before fire occurrence. Step 2 starts a search for initial seed pixels with low NIR that may be areas where the forest fires began in the later image after fire occurrence. Adaptive thresholds were calculated in step 3 using the CDFs from burned and unburned pixels' statistics. Step 4 performs region growing segmentation using the seed pixels to mimic the direction forest fires may have spread. Last in step 5, post processing is implemented to remove areas that may be too large as compared to the distribution of burned seed pixels. The study areas chosen are located in New South Wales, Australia. About 62% of all vegetation with history of recent fire in NSW are now under threat from too much burning and only 13% are within thresholds. The increased frequency of fire caused by lighting as seen during the "Black Summer" bushfire season of 2019 to 2020 occurred in more remote and inaccessible areas (NSW EPA, 2021). Remote sensing using satellite images can hence help to monitor these large areas from above the ground, providing a bird's eye view with a wide extent. Results showed that more than 95% of the burned areas in both study areas can be detected. Large and small burned areas can be delineated and be considered for further studies into fire recovery works and monitoring of forest regrowth rates at the regional or local scale. High spatial resolution 0.8m 4 bands TripleSat images are indeed capable of extracting large and small burned areas in the region of interest.

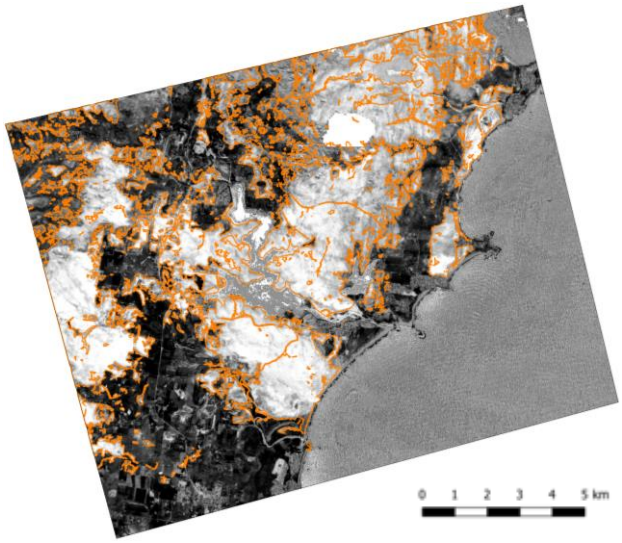

a) TripleSat burned area result for study area 1 overlaid on NBR result using Sentinel 2

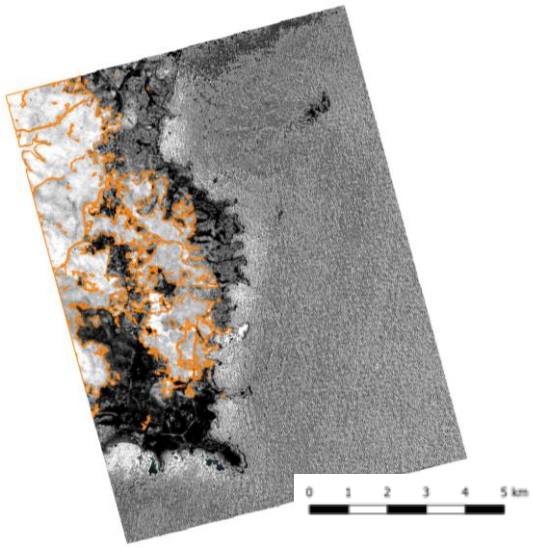

b) TripleSat burned area result for study area 2 overlaid on NBR result using Sentinel 2

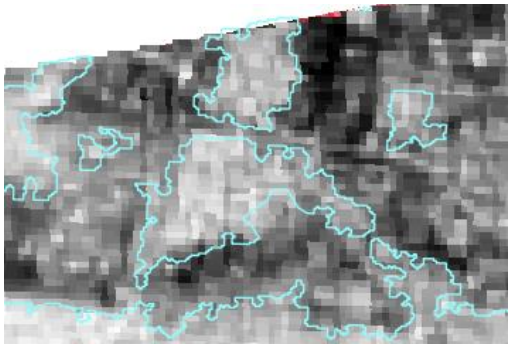

c) Small polygon burned area TripleSat result overlaid on NBR result using Sentinel 2

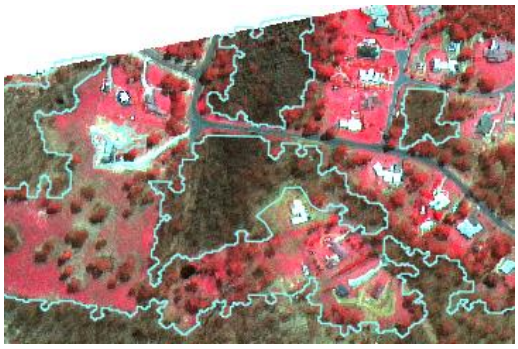

d) Small polygon burned area TripleSat result overlaid on false colour TripleSat image

Figure 6. Comparison of TripleSat results with Sentinel 2's NBR results

REFERENCES

21AT, 2023. TripleSat Constellation. Twenty First Century Aerospace Technology (Asia) Pte. Ltd. https://www.21at.sg/productsservices/triplesat-constellation/

Campagnolo, M.L., Libonati, R., Rodrigues, J.A. and Pereira, J.M.C., 2021. A comprehensive characterization of MODIS daily burned area mapping accuracy across fire sizes in tropical savannas. *Remote Sensing of Environment*. 252, 112115. https://doi.org/10.1016/j.rse.2020.112115

Canadell, J.G., Meyer, C.P., Cook, G.D., Dowdy, A., Briggs, P.R., Knauer, J., Pepler, A. and Haverd, V., 2021. Multi-decadal increase of forest burned area in Australia is linked to climate change. *Nature Communications*. 12, 6921. https://doi.org/10.1038/s41467-021-27225-4

Chuvieco, E., Mart, M. and Palacios-Orueta, A., 2002. Assessment of different spectral indices in the red-near-infrared spectral domain for burned land discrimination. *International Journal of Remote Sensing*. 23, pp. 5103-5110. https://doi.org/10.1080/01431160210153129

Chuvieco, E., Mouillot, F., R. van der Werf, G., Miguel, J.S., Tanase, M., Koutsias, N., García, M., Yebra, M., Padilla, M., Gitas, I., Heil, A., Hawbaker, T.J. and Giglio, L., 2019. Historical background and current developments for mapping burned area from satellite Earth observation. *Remote Sensing of Environment*. 225, pp. 45-64. https://doi.org/10.1016/j.rse.2019.02.013

Cui, Y., Liu, M. and Li, S., 2020. Emergency monitoring and post-disaster reconstruction monitoring in the tornado disaster in Yancheng, Jiangsu. Proc. SPIE 11432, MIPPR 2019: Remote Sensing Image Processing, Geographic Information Systems, and Other Applications, 1143212. https://doi.org/10.1117/12.2538181

Gärtner, P., Förster, M., Kurban, A. and Kleinschmit, B., 2014. Object based change detection of Central Asian Tugai vegetation with very high spatial resolution satellite imagery. *International Journal of Applied Earth Observation and Geoinformation*. 31, pp. 110-121. https://doi.org/10.1016/j.jag.2014.03.004

Guliaeva, S.I., Bruchkousky, I.I. and Katkovsky, L.V., 2021. Determining the Drying Out of Coniferous Trees Using Airborne and Satellite Data. *Advances in Remote Sensing*. 10, pp. 25-46. https://doi.org/10.4236/ars.2021.102002

Hoover, K. and Hanson, L.A., 2023. Wildfire Statistics. Congressional Research Service. https://sgp.fas.org/crs/misc/IF10244.pdf

Lizundia-Loiola, J., Otón, G., Ramo, R. and Chuvieco, E., 2020. A spatio-temporal active-fire clustering approach for global burned area mapping at 250 m from MODIS data. *Remote Sensing of Environment*. 236. https://doi.org/10.1016/j.rse.2019.111493

Llorens, R., Sobrino, J.A., Fernández, C., Fernández-Alonso, J.M. and Vega, J.A., 2021. A methodology to estimate forest fires burned areas and burn severity degrees using Sentinel-2 data. Application to the October 2017 fires in the Iberian Peninsula. *International Journal of Applied Earth Observation and Geoinformation*. 95. https://doi.org/10.1016/j.jag.2020.102243

MacCarthy, J., Richter, J., Tyukavina, S., Weisse, M. and Harris, N., 2023. The Latest Data Confirms: Forest Fires Are Getting Worse. World Resources Institute. https://www.wri.org/insights/global-trends-forest-fires#:~:text=Though%20down%20from%20the%20previous,and%20catastrophic%20fires%20in%20Hawaii.

NSW EPA, 2021. Fire. NSW State of the Environment 2021 (SoE 2021), NSW Environment Protection Authority. https://www.soe.epa.nsw.gov.au/all-themes/land/fire#areaburnt

Panuju, D.R., Paull, D.J. and Griffin, A.L., 2020. Change Detection Techniques Based on Multispectral Images for Investigating Land Cover Dynamics. *Remote Sensing.* 12(11), 1781. https://doi.org/10.3390/rs12111781

Pereira, J. M. C., 1999. A comparative evaluation of NOAA/AVHRR vegetation indexes for burned surface detection and mapping. *IEEE Transactions on Geoscience and Remote Sensing*. 37(1), pp. 217-226. https://doi.org/10.1109/36.739156

Pleniou, M. and Koutsias, N. 2013. Sensitivity of spectral reflectance values to different burn and vegetation ratios: A multi-scale approach applied in a fire affected area. *ISPRS Journal of Photogrammetry and Remote Sensing*. 79, pp. 199-210. https://doi.org/10.1016/j.isprsjprs.2013.02.016

Qi, W., 2022. Object detection in high resolution optical image based on deep learning technique. *Natural Hazards Research*. 2(4), pp. 384-392. https://doi.org/10.1016/j.nhres.2022.10.002

Stroppiana, D., Bordogna, G., Carrara, P., Boschetti, M., Boschetti, L. and Brivio, P.A., 2012. A method for extracting burned areas from Landsat TM/ETM+ images by soft aggregation of multiple Spectral Indices and a region growing algorithm. *ISPRS Journal of Photogrammetry and Remote Sensing*. 69, pp. 88-102. https://doi.org/10.1016/j.isprsjprs.2012.03.001

Uddin, K., Gilani, H., Murthy, M. S. R., Kotru, R. and Qamer, F.M., 2015. Forest Condition Monitoring Using Very-High-Resolution Satellite Imagery in a Remote Mountain Watershed in Nepal. *Mountain Research and Development*. 35(3), pp. 264-277. https://doi.org/10.1659/MRD-JOURNAL-D-14-00074.1

USGS, 2023. Landsat Collection 2 Level-3 Burned Area Science Product. U.S. Geological Survey, Fact Sheet 2022–3083. https://pubs.usgs.gov/fs/2022/3083/fs20223083.pdf

WWF. 2020. Fires, forests and the future: A crisis raging out of control?. World Wide Fund for Nature & Boston Consulting Group. https://wwfeu.awsassets.panda.org/downloads/wwf_fires_forests_and_the_future_report.pdf

WWF. 2020. Why forests are so important. World Wide Fund for Nature. https://wwf.panda.org/discover/our_focus/forests_practice/importance_forests/

Zubieta, R., Ccanchi, Y. and Liza, R. 2023. Performance of heat spots obtained from satellite datasets to represent burned areas in Andean ecosystems of Cusco, Peru. *Remote Sensing Applications: Society and Environment*. 32, 101020. https://doi.org/10.1016/j.rsase.2023.101020